2003 Pacific Conference on Earthquake Engineering

Displacement of gravity retaining walls under seismic loading

M. Okamura, Y. Saito, K. Tamura

Public Works Research Institute, Tsukuba-shi, 305-8516, Japan.

O. Matsuo

National Institute for Land and Infrastructure Management, Tsukuba-shi, 305-0804, Japan.

ABSTRACT: This paper describes a new calculation method for seismic displacement of retaining walls with embedment. A macroscopic failure surface and a plastic displacement potential in the general load space are considered in the method to evaluate the subgrade reaction force from foundation ground. The method is capable of calculating not only horizontal, vertical or rotational displacement alone, but also their combined effect. The method is validated through comparison with centrifuge test results of a gravity retaining wall with dense backfill sand subjected to strong base shaking. The calculated displacement components, that is vertical, horizontal and rotational displacement, agreed well with those measured.

1 INTRODUCTION

There is an apparent trend to switch over to design of earth structures based on a specified limit displacement in recent years. Analytical methods to estimate the displacement under seismic loading have increased in importance. In order to estimate earthquake-induced displacement of retaining walls, several practical calculation methods have been developed. Most of the methods are based on the sliding block analogy originally developed by Newmark (1965) and they are only applicable to a single degree-of-freedom problem to calculate sliding displacement or rotation alone (Richards and Elms, 1979; Richards et al., 1996; Zeng and Steedman, 2000). These methods essentially involve two major problems;

(1) Generally the movements of retaining walls in reality cannot result from purely sliding, subsidence or rotation but their combined effect. Since horizontal displacement at the top of walls can be one of the determining factors of the integrity of structures on the backfills, not only the sliding displacement but also rotation should be considered to be of primary importance in design practice,

(2) In these methods, a one directional motion or failure mechanism is considered (mostly sliding failure mechanism). The frictional force on the wall base to resist the wall movement assumed in the methods is,

$$H = m \times V \tag{1}$$

where m is the friction coefficient between the soil and the wall base and V is vertical force on the base. Although equation (1) holds true only when the foundation soil can be regarded as rigid, or V is very small as compared with the bearing capacity of the foundation soil, most methods based on the sliding block analogy adopt this assumption about the frictional force H. Since the frictional force is one of the influential factors determining the displacement of walls, H must be determined carefully.

Okamura and Matsuo (2002) indicated that equation (1) considerably overestimates the frictional force for actual retaining walls. This suggests the possibility of calculated displacement using the assumption of equation (1) being on the unsafe side. A more realistic frictional force instead of

$H=mV$ is needed for more accurate displacement predictions.

Okamura and Matsuo (2002) recently developed a method to calculate fully coupled displacement, that is vertical, horizontal and rotational displacement, of retaining walls without embedment under earthquake loading using more realistic subgrade reactions acting on the wall base. In this paper we extended the method so that it can be applied to retaining walls with embedment. The method is validated through comparison between calculation results and centrifuge test observations.

2 BEARING CAPACITY ENVELOPE AND PLASTIC DISPLACEMENT POTENTIAL FOR FOUNDATION WITH EMBEDMENT

In order to predict behavior of retaining walls which undergo combined vertical (V), horizontal (H) and moment (M) loading, the response of the ground supporting a wall to this combined loading must be well understood.

2.1 Failure envelope

For a rigid foundation on a level ground, the failure envelope of the ground in a V-H-M/B general load space has been analyzed and many investigators have proposed mathematical expressions of the envelope (Georgiadis and Butterfield, 1988; Nova and Montrasio, 1991; Gottardi and Butterfield, 1993; Butterfield and Gottardi, 1994; Bransby and Randolph, 1998; Ukritchon et al., 1998; Martin and Houlsby, 2000; Okamura et al., 2002). To preserve dimensional homogeneity the moment, M is divided by the foundation width, B. One of the simplest expressions of the failure envelope is of the form shown in Fig. 1 and equation (2) (Butterfield and Gottardi, 1994), which has been termed a 'cigar shaped envelope'.

$$\left(\frac{H}{mV_{\max}}\right)^2+\left(\frac{M}{jBV_{\max}}\right)^2-\frac{2CHM}{mjB}=\left(1-\frac{V}{V_{\max}}\right)^2\left(\frac{V}{V_{\max}}\right)^2 \qquad (2)$$

$$C=\tan 2r\,\frac{(m-j)(m+j)}{2mj}$$

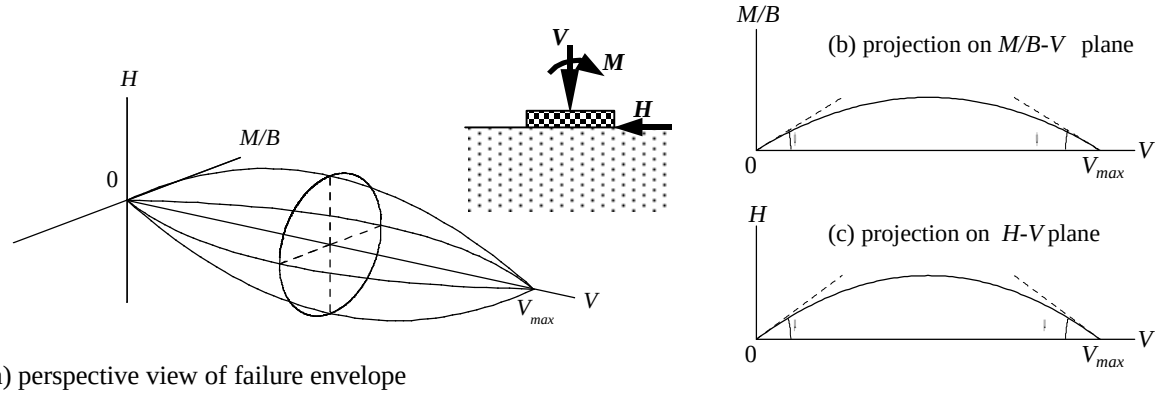

(a) perspective view of failure envelope

Figure 1. Failure envelope in general load space (after Butterfield and Gottardi, 1994)

The symbols V, H and M are the total vertical and horizontal force and moment sustained by the ground, thus the subgrade reaction forces. The reference point of the moment is the center of the foundation base. Fig.1 (b) and (c) show the cross sections of the failure envelope in the M/B-V plane (H = 0) and in the H-V plane (M = 0) to be parabolas which intersect the V axis at V = 0 and $V = V_{max}$, where the tangential slopes are either j or m, and V_{max} is the maximum vertical load capacity for the central vertical loading ($H = M = 0$) for a particular embedment depth. The constant m is the friction coefficient at the foundation base. The cross section of the failure envelope in M/B-H plane at a constant V is an ellipse with an axis ratio of m/j, which is rotated at an angle r around the center of the ellipse. For a footing resting on the ground surface, that is the footing without embedment, many

experimental data is available in the literature to determine the complete failure envelope in the *V-H-M/B* general load space, however, data is very limited with regard to footings with embedment. In this study a series of bearing capacity tests was conducted to obtain supplemental data on the effect of embedment depth on the failure envelope.

2.2 **Bearing capacity tests on footing with embedment**

Dry Toyoura sand (D_{50}= 0.19 mm, G_s= 2.640, e_{max}= 0.973 and e_{min}= 0.609) was rained to a depth of about 200 mm at a relative density Dr = 84 % from a hopper into a rigid model container with internal dimensions of 800 mm long, 200 mm wide and 300 mm deep. A 40 mm wide strip footing with rough base was placed as shown in Fig.2. In order to make sure that the footing was free to rotate at the loading point, the load from loading jack was applied to the footing through a ball bearing. The ball bearing was set at a distance e_i from the center as shown in Fig.2. The normal and shear load applied to the footing was measured with a load cell.

The testing parameters in this study are the embedment depth of the footing and the eccentricity and the inclination of applied load. The load inclination a varied from 0 to 35° at an interval of 5 °, the initial load eccentricity e_i , ranged from 0 (central loading) to 12 mm at an interval of 2 mm. Three embedment depths of footing, D= 0, 7 and 20mm (D/B= 0, 0.17 and 0.5) were selected, where B= footing breadth. A total of 52 tests were conducted.

Relationships between vertical and moment load (V, M/B) at failure normalized with respect to the maximum vertical load V_{max} are plotted in Fig.3, together with least-square-fit parabolas given by equation (3). Also shown in Fig.3 is the similar plot on the H-V plane with parabolas expressed as equation (4). These equations were derived from equation (2) by substituting H= 0 or M= 0.

$$\frac{M}{BV_{\max}} = j\,\frac{V}{V_{\max}}\left(1-\frac{V}{V_{\max}}\right) \qquad (3)$$

$$\frac{H}{V_{\max}} = m\,\frac{V}{V_{\max}}\left(1-\frac{V}{V_{\max}}\right) \qquad (4)$$

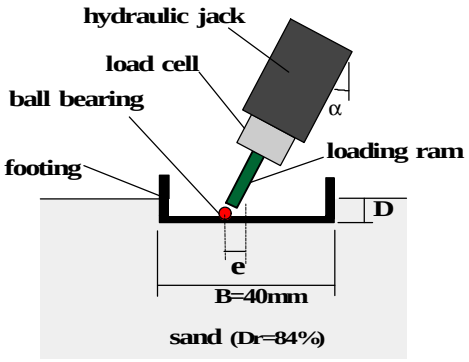

Figure 2. Schematic illustration of setup for bearing capacity test.

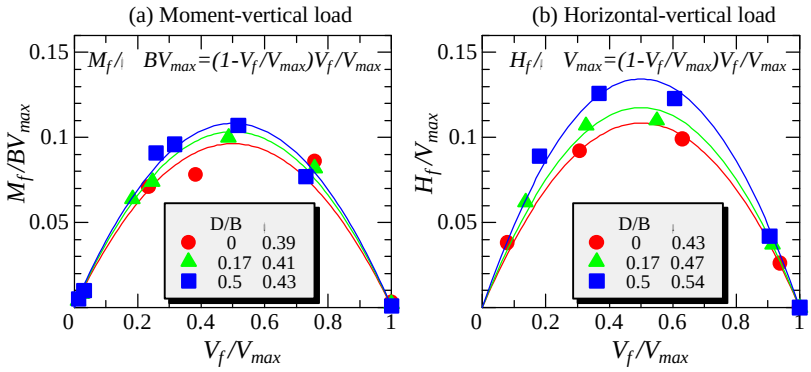

Figure 3. Failure loci on normalized load plane.

It can be observed that the maximum moment occurred at about half the maximum vertical load and the parabolas can provide reasonably good fit to the data points, and thus the failure locus.

Figure 4 represents the plot of the moment versus horizontal load at failure for three embedment depths. In order to plot all the test results in this figure, both abscissa and ordinate are divided by (1-V_f/V_{max}). Ellipses in the figure were also derived from equation (2) with the use of parameters j and m shown in Fig.3. Rotation angles of the ellipses, r, in the figure were determined by least-square-fit to the data points. The angle r seems to be constant irrespective of embedment depth. It can be concluded that equation (2) provides a good approximation of failure envelope of shallow foundation on dense sand bed.

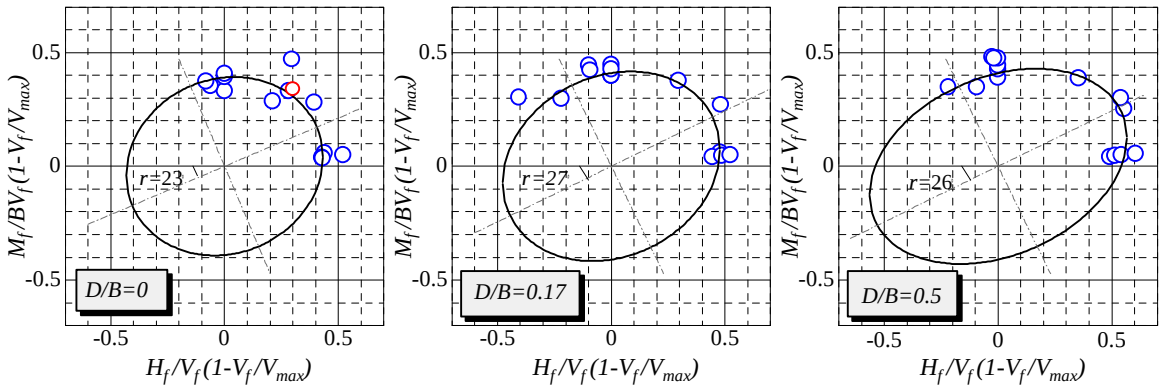

Figure 4. Failure loci on normalized moment- horizontal load plane for different embedment depth

The variations of three parameters in equation (2) with *D/B* are given in Fig.5. It can be seen that both j and m increased with embedment depth.

2.3 **Plastic displacement potential**

In order to describe the displacement characteristics of foundations under combined loading, the flow rule has been examined, in which a macroscopic constitutive law for the entire soil-foundation system was considered. Associated plasticity is often assumed so that the failure envelope also describes the plastic displacement potential defining the relative magnitudes of the incremental plastic displacement during failure. But the associated flow rule significantly overestimates vertical displacement in the upward direction especially when the vertical load is lower than $V_{max}/2$ (Gottardi and Butterfield, 1995; Bransby and Randolph, 1998; Martin and Houlsby, 2000; Okamura et al., 2002). The plastic displacement potential, *Q*, used in this study was determined based on the model test results by Georgiadis and Butterfield (1988) and Okamura et al. (2002) as shown in Fig.6 and equation (5). It should be noted here that data which can be used to determine the plastic potential is apparently scarce in the literature, accumulation of experimental data and revision of the plastic displacement potential is needed.

$$Q = \sqrt{\left(\frac{H}{mV_{\max}}\right)^2 + \left(\frac{M}{jBV_{\max}}\right)^2} + 0.44\left(\frac{V}{V_{\max}}\right)^2 - 0.44 = 0 \qquad (5)$$

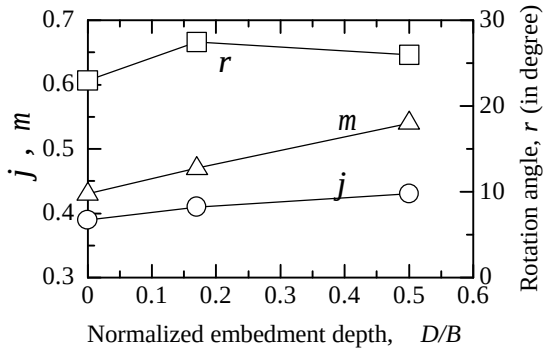

Figure 5. Variation of parameters for failure

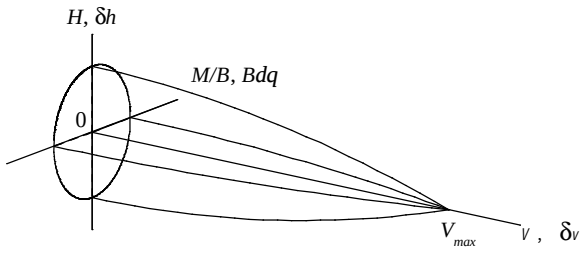

Figure 6. Perspective view of plastic displacement

3 **METHOD OF CALCULATION**

The important aspect of the bearing capacity characteristics under combined loading discussed in the preceding section is that the subgrade reaction force during failure is located on the failure envelope and its location on the envelope is determined by the flow rule with the incremental displacement

vector or velocity vector of the foundation as conceptually illustrated in Fig. 7. In this section, the computational procedure for retaining wall displacement during an earthquake is briefly described, which incorporates the subgrade reaction based on the failure envelope in the general load space and the flow rule illustrated in the previous section. More detailed information about this method can be found elsewhere (Okamura and Matsuo, 2002).

3.1 **Basic assumptions**

Some basic assumptions are made as follows.

(a) First, the failure envelope of the ground in the load space can be defined as

$$F = F(V, H, M/B) = 0 \tag{6}$$

(b) Second, in a manner typical of sliding block analysis, the foundation soil is assumed to be a rigid-perfectly plastic media. The subgrade reaction forces (*V, H, M/B*) have to be within the failure envelope ($F < 0$) or on the failure envelope ($F = 0$).

(c) Third, a further assumption regarding the direction of incremental plastic displacement must be made. In a manner consistent with the theory of plasticity, in which the ratio of incremental plastic strain is related to the state of stress, "plastic displacement potential", *Q*, is defined. The incremental displacement vector in the work-conjugate displacement space, $\dot{s}$, is assumed to be orthogonal to the plastic displacement potential. Thus we have,

$$\dot{s} = \{dv, dh, Bdq\} = l \frac{\partial Q}{\partial R} \tag{7}$$

in which v and h are vertical and horizontal displacements at the center of wall base relative to the foundation ground, q is rotation, $R = \{V, H, M/B\}$ is the subgrade reaction vector and l is a constant. These assumptions indicate that when the wall is moving, the ground is in the failure condition and the vector *R* is determined by the following two conditions:

(i) *R* is on the failure envelope ($F = 0$), and

(ii) the vector $\dot{s}$ is normal to the plastic displacement potential.

3.2 **Computational procedure**

Consider a retaining wall resting on a ground having the failure envelope and plastic displacement potential in the form of equations (2) and (5), which subjects to an external load at time *t*, $E_{(t)} = \{V_{e(t)}, H_{e(t)}, M_{e(t)}/B\}$. The external load, *E*, includes all the loads acting on the wall except for the subgrade reaction force on the base, such as the earth thrust from the backfill and the self weight and the inertial force of the wall. The flow of computational steps is shown in Fig. 8.

The necessary input data for this calculation includes a bearing capacity force for vertical central loading (V_{max}), width of the base *B*, mass *m* and polar moment of inertia *I* of the wall, and the earth thrust from the backfill and ground acceleration time histories. It has been reported that the constants j and m do not change significantly with the relative density of sand and scale of the foundation but stay in a relatively narrow range between 0.35 and 0.45 for strip foundations (Okamura et al., 2002).

4 **VERIFICATION OF THE METHOD**

The proposed method was utilized to simulate a centrifuge model of a gravity retaining wall subjected to base shaking (Nakamura et al., 2001). In this section, the centrifuge model is briefly reviewed first and then the method is verified through the comparison of computational results with the model test data.

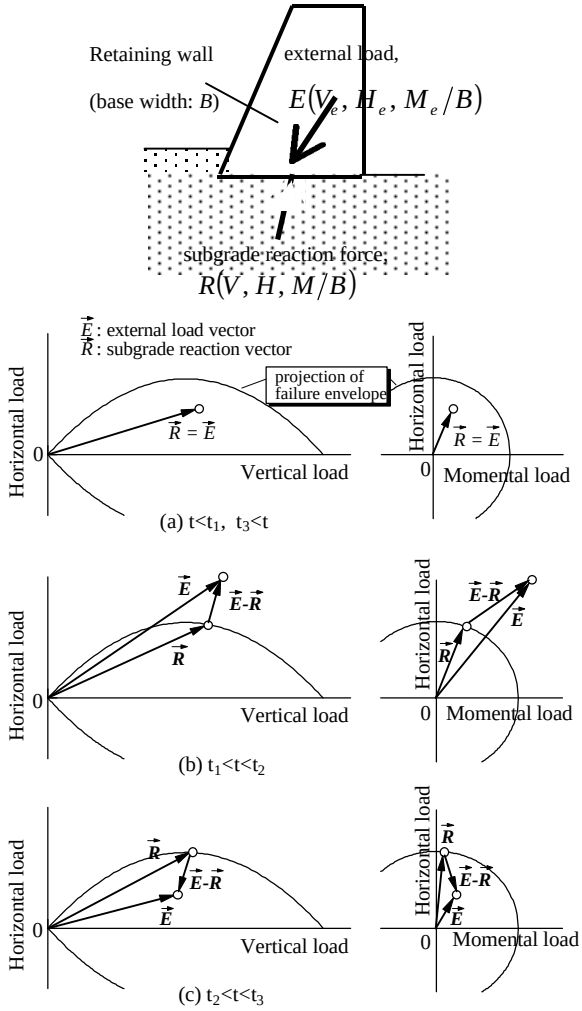

Figure 7. External load and subgrade reaction vectors on load space

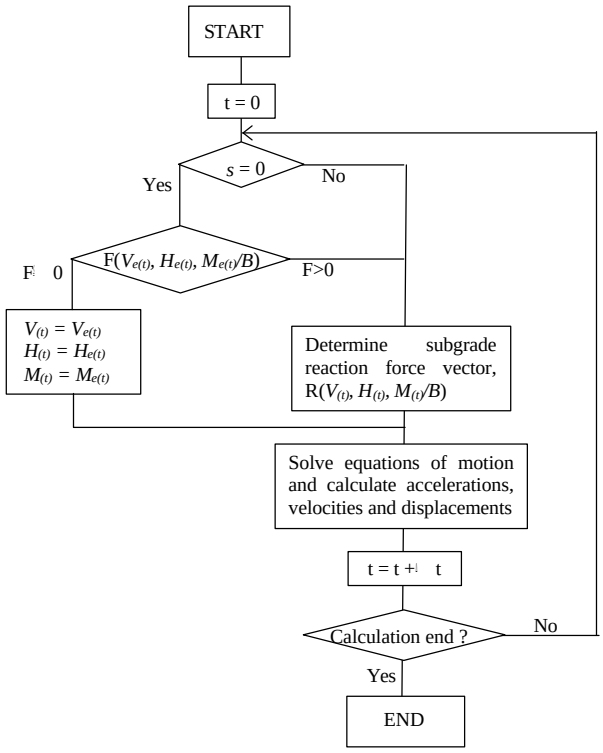

Figure 8. Flow of computational procedures

4.1 **Centrifuge test**

Centrifuge tests on the seismic behavior of a gravity retaining wall on a dry, dense sand bed were conducted. Fig. 9 sketches a side view of the plane strain model prepared in a rigid model container. The bed and the backfill were prepared by raining dry Toyoura sand to a relative density of 85 %. The angle of shear resistance of the sand, f', obtained from plane strain compression tests under a confining pressure of 98 kPa was 45 degrees. The model retaining wall had dimensions of 15 cm wide by 30 cm high, and was composed of stainless steel plates and built-in earth pressure cells so that the distributions of normal and shear stresses on the base and the back could be measured. The total mass of the wall per unit length was 59.3 kg/m, giving rise to a safety factor against static bearing capacity failure of about 20. The height of the center of gravity and the polar moment of inertia of the center of gravity were 12.6 cm above the base and 0.340 kg$\,$m^2, respectively. Three models were tested with different embedment depths of D/B= 0, 0.2 and 0.4.

Shaking tests were conducted at 30 G centrifugal environment. The model container was excited by 25 cycles of a 45 Hz simulated sinusoidal input parallel to the base of the container with uniform acceleration amplitude. The shaking event was repeated several times, separated by ample time interval, with varying acceleration amplitude from 4.2 G to 21 G. The corresponding prototype is the 9.0 m high retaining wall subjected to a sinusoidal base acceleration time history of about 0.14 G to 0.69 G peak acceleration and of 1.5 Hz frequency. More detailed information regarding the tests can be found in Matsuo et al. (2002). In the following discussion, all comparisons are made in prototype units otherwise mentioned.

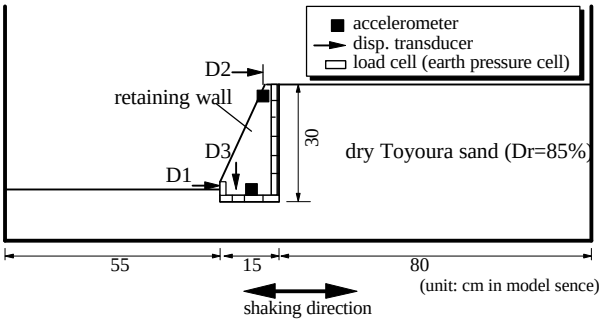

Figure 9. Centrifuge model setup

4.2 **Comparisons with computational results**

The failure envelope and the plastic displacement potential specified by equations (2) and (5) were used in the calculation. The constants in those equations, m, j and r, used in the calculation are shown in Table 1. These values were determined based on the experimental results described in the preceding section, taking the scale effect of foundation (Okamura et al., 2002) into account. External loads and moment around the center of the wall base due to the inertia of the wall and earth pressure from the backfill were evaluated from the measured input acceleration records and the records of normal and shear pressures acting on the back of the wall.

Table 1 Parameters of failure envelope

D/B	m	j	r
0	0.50	0.45	25 degree
0.2	0.55	0.47	
0.4	0.59	0.48	

In reality the increase in rotation results in a higher overturning moment (Richards et al., 2000). The influence of rotation of the wall on the overturning moment was taken into account in the calculation by updating the location of the center of gravity of the wall.

The input base acceleration and measured displacement time histories of the model without embedment are depicted in Fig. 10 with those calculated from the proposed method. It should be noted that ordinate for the vertical displacement is exaggerated in the figure because the settlement of the wall was much smaller than horizontal displacement. Vertical, horizontal and rotational displacements calculated from the method agreed well with those from the test.

Figure 11 depicts horizontal displacement and rotation of the walls accumulated during each shaking event plotted against input acceleration amplitude. It can be observed from Fig.11(a) that both horizontal displacement and rotation increased with the input acceleration. The threshold acceleration above which displacement and rotation started to accumulate was about 0.3G for the wall without embedment and 0.45G for the wall with D/B= 0.4. The threshold acceleration obtained from the calculation agreed quite well with the test observations. Calculated displacement and rotation also compared well with test results for cases with shallower embedment depth, but tended to overestimate both the horizontal and rotational displacement for the case with D/B= 0.4. A possible reason for this discrepancy between experimental observation and analytical results is that the failure envelope employed in this study pass through the origin of the general load space; passive earth thrust on the front of the wall is expected in reality but equation (2) yields H= 0 at V=0.

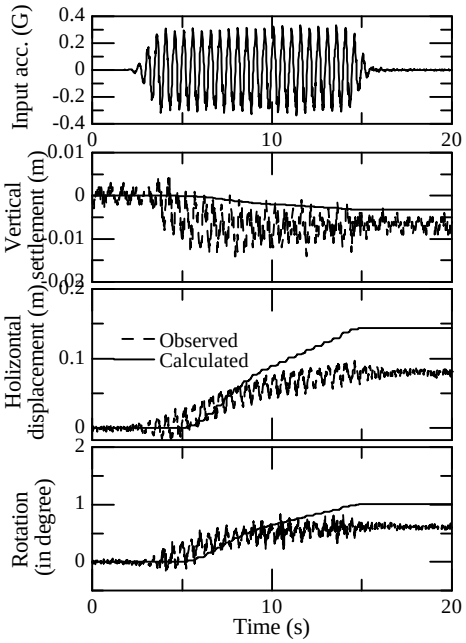

Figure 10. Input acceleration and displacement of wall without embedment.

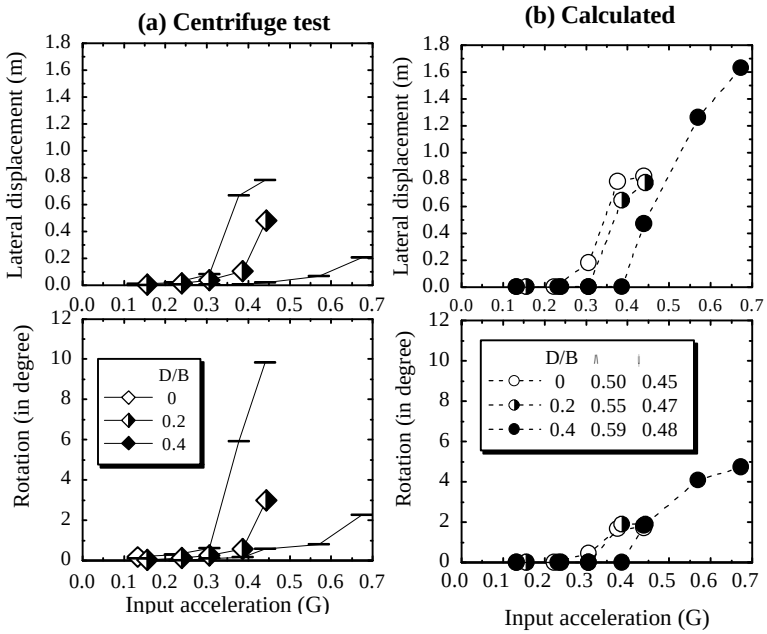

Figure 11. Horizontal displacement and rotation angle of retaining wall accumulated in each shaking event.

Another possible cause for the above mentioned differences is the plastic displacement potential and the failure envelope used in the calculation. Most footing tests conducted so far aimed at investigating overall shape of failure envelope and plastic displacement potential, so that information about the failure envelope and the plastic displacement potential in the vicinity of the origin in the general load space was scarce. In fact, the ratio of external vertical load to V_{max} in this example calculation was considerably small, therefore, different value of the constants m and j might be more appropriate.

There may be a need to modify plastic displacement potential and failure envelope used in the calculation, however, above discussions lead authors to a conclusion that if the earth thrust from backfill is appropriately given, the proposed method could be one of the effective tools to assess fully coupled displacement of retaining walls with shallower embedment depth. Discussion about the evaluation method of the earth thrust from backfill can be found elsewhere (Nakamura et al., 2001).

5 SUMMARY

This paper proposed a new calculation method for seismic displacement of retaining walls with and without embedment. A macroscopic failure surface and plastic displacement potential in the general load space were considered in the method to evaluate the subgrade reaction forces from foundation ground. The method is capable of calculating not only horizontal but also vertical and rotational displacements simultaneously.

The method has been validated by comparison with dynamic centrifuge test results of a retaining wall. The method tends to overestimate displacement to some extent as embedment depth increases, however, the method can be one of the effective tools to assess fully coupled displacement of retaining walls.

REFERENCES:

Bransby, M. F. and Randolph, M. F. (1998): Combined loading of skirted foundations, *Geotechnique* 48(5), 637-655

Butterfield, R. and Gottardi, G. (1994): A complete three-dimensional failure envelope for shallow footings on sand, *Geotechnique* 44(1), 181-184

Georgiadis, M. and Butterfield, R. (1988): Displacements of footings on sand under eccentric and inclined loads, *Canadian Geotechnical Journal* 25(1), 199-212

Gottardi, G. and Butterfield, R. (1993): On the bearing capacity of surface footings on sand under general planar loads, *Soils and Foundations* 33(3), 68-79

Gottardi, G. and Butterfield, R. (1995): The displacement of a model rigid surface footing on dense sand under general planar loading, *Soils and Foundations* 35(3), 71-82

Martin, C. M. and Houlsby, G. T. (2000): Combined loading of spudcan foundations on clay: laboratory tests, *Geotechnique* 50(4), 325-338

Matsuo, O., Nakamura, S. and Saito, Y. (2002): Centrifuge tests on seismic behaviour of retaining walls, *Proc. Int. Conf. Physical Modelling in Geotechnics*, 453-458

Nakamura, S., Saito, Y. and Matsuo, O. (2001): Seismic behavior of gravity retaining walls and prediction of displacement (part 6), *Proc. 56th Annual Conf. Japan Society of Civil Engneers*, 3-A, 240-241

Newmark, N. M.(1965): Effects of earthquakes on dams and embankments, *Geotechnique* 15(2), 139-160

Nova, R. and Montrasio, L. (1991): Settlements of shallow foundations on sand, *Geotechnique* 41(2), 243-256

Okamura, M., Mihara, A., Takemura, J. and Kuwano, J. (2002): Effects of footing size and aspect ratio on the bearing capacity of sand subjected to eccentric loading, *Soils and Foundations*, 42(4), 43-56

Okamura, M. and Matsuo. O. (2002): A displacement prediction method for retaining walls under seismic loading, *Soils and Foundations*, 42(1), 131-138

Richards, R. and Elms, D. G. (1979): Seismic behavior of gravity retaining walls, *Journal of Geotechnical Engineering*, ASCE, 105(4), 449-469

Richards, R., Fishman, K. and Divito, R. C. (1996): Threshold acceleration for rotation and sliding of bridge abutments, *Journal of Geotechnical and Geoenvironmental Engineering*, ASCE, 112(9), 752-759

Ukritchon, B., Whittle, A. J. and Sloan, S. W. (1998): Undrained limit analyses for combined loading of strip footings on clay, *Journal of Geotechnical and Geoenvironmental Engineering*, ASCE, 124(3), 265-276

Zeng, X. and Steedman, R. S. (2000): Rotational block method for seismic displacement of gravity walls, *Journal of Geotechnical and Geoenvironmental Engineering*, ASCE, 126(8), 709-717